Available online at www.sciencedirect.com
SCIENCE DIRECT®
Carbohydrate Research 340 (2005) 59–68
Carbohydrate RESEARCH

Structural analysis of the lipopolysaccharide of *Pasteurella multocida* strain VP161: identification of both Kdo-P and Kdo–Kdo species in the lipopolysaccharide

Frank St. Michael,[a] Jianjun Li,[a] Evgeny Vinogradov,[a] Suzon Larocque,[a] Marina Harper[b] and Andrew D. Cox[a,*]

[a]*Institute for Biological Sciences, National Research Council, Ottawa, ON, Canada K1A 0R6*
[b]*Australian Bacterial Pathogenesis Program, Department of Microbiology, Monash University, VIC 3800, Australia*

Received 14 July 2004; accepted 20 October 2004
Available online 18 November 2004

Abstract—The structure of the lipopolysaccharide from the *Pasteurella multocida* strain VP161 was elucidated. The lipopolysaccharide was subjected to a variety of degradative procedures. The structures of the purified products were established by monosaccharide and methylation analyses, NMR spectroscopy and mass spectrometry. The following structures for the lipopolysaccharides were determined on the basis of the combined data from these experiments.

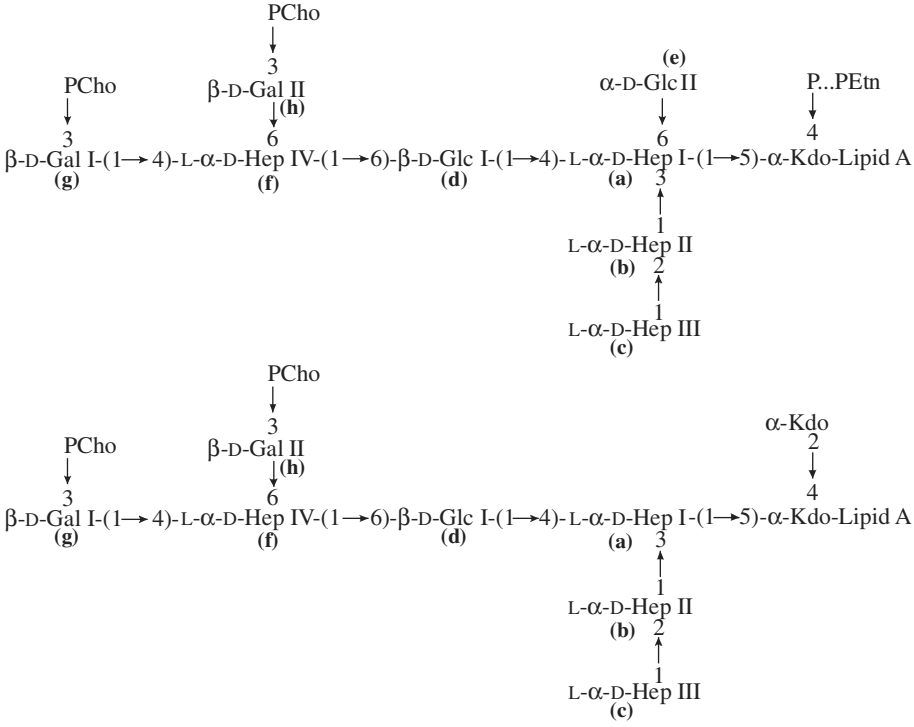

* Corresponding author. Tel.: +1 613 991 6172; fax: +1 613 952 9092; e-mail: andrew.cox@nrc-cnrc.gc.ca

0008-6215/$ - see front matter
doi:10.1016/j.carres.2004.10.017

Based on the NMR data, all sugars were found in pyranose ring forms, and Kdo is 2-keto-3-deoxy-octulosonic acid, L-α-D-Hep is L-*glycero*-D-*manno*-heptose, PPEtn is pyrophosphoethanolamine and PCho is phosphocholine. Intriguingly, when the O- and fully deacylated LPS was examined, it was evident that there was variability in the arrangement of the Kdo region of the molecule. Glycoforms were found with a Kdo-P moiety, as well as glycoforms elaborating a Kdo–Kdo group. Furthermore the Glc II residue was not attached to Hep I when two Kdo residues were present, but it was attached when the Kdo-P arrangement was elaborated, suggesting a biosynthetic incompatibility due to either steric hindrance or an inappropriate acceptor conformation. This variation in the Kdo region of the LPS was also observed in several other *Pasteurella multocida* strains investigated including the genome strain Pm70.

Keywords: *Pasteurella multocida*; LPS; Core oligosaccharide; Mass spectrometry; NMR spectroscopy

1. Introduction

Pasteurella multocida (*Pm*) is a Gram-negative bacterium and multi-species pathogen that causes serious diseases in food animals and humans. This bacterium is the causative agent of fowl cholera in chickens and turkeys,[1] haemorrhagic septicaemia in cattle,[2] atrophic rhinitis in pigs[3] and dog and cat bite infections in humans.[4] Several *Pm* virulence factors have previously been identified, including the capsule in serogroups A and B,[5] and LPS.[6] However, there are conflicting reports as to the endotoxic properties of LPS isolated from *Pm*. LPS isolated from a serotype B:2 strain was shown to be endotoxic, and intravenously administered LPS could reproduce clinical signs of haemorrhagic septicaemia in buffalo.[7] However, turkey poults were found to be relatively resistant to the lethal effects of LPS isolated from serogroup A strains of *Pm*, although the inflammatory response and microscopic hepatic lesions were similar to those observed in mammalian hosts.[8,9] In contrast, chicken embryos and mice were found to be highly susceptible to the toxic effects of *Pm* LPS.[10]

Pm strains are classified into Heddleston serotypes based on the antibody responses to LPS, whilst antibodies raised against heat-killed *Pm* vaccines are primarily directed against LPS and protect the host against strains within the same serotype.[11] Early studies demonstrated that LPS purified using the hot phenol–water method and injected into mice and rabbits resulted in a poor antibody response and no protection against *Pm* infection; however, the same LPS when injected into chickens induced a good antibody response that passively protected recipients against disease.[12] Monoclonal antibodies raised against the LPS from a serotype A strain were shown to be bactericidal and to completely protect mice against homologous challenge.[13] In addition, an opsonic monoclonal antibody against a serotype B strain of *Pm* LPS was shown to partially protect mice against *Pm* infection.[14]

A modified LPS structure clearly affects the viability of *Pm* in vivo. Recently three strongly attenuated mutants of *Pm* strain VP161 were identified where each had a single transposon insertion in the gene *pm1294* (designated $waaQ_{PM}$).[15] This gene was subsequently shown to encode a heptosyltransferase, the mutation of which resulted in a highly truncated LPS structure.[16] Furthermore, a *Pm galE* mutant has been constructed previously and was attenuated in mice, although no structural analysis of the LPS was reported.[17] *Pm* isolates may be grouped serologically based on their capsular antigens into five serogroups A, B, D–F using a passive haemaglutination test with erythrocytes sensitised with capsular antigen. Structural information is available for the capsules of serogroups A (hyaluronic acid),[18] D (heparin) and F (chondroitin),[19] each being an example of the well-studied glycosaminoglycans. Somatic (LPS) typing can also be used for the identification of strains, and there have been two main systems reported. The Namioka system is based on a tube agglutination test and is able to recognise 11 serotypes,[20] whereas the Heddleston system using a gel-diffusion precipitation test can recognise 16 serotypes and is currently the preferred method.[21]

In 1981 a standard system for the identification of *P. multocida* serotypes was recommended that utilised both the Carter capsular typing identified by the letters A, B, D, E and F, and the Heddleston somatic typing system identified by numbers.[22] *Pm* expresses LPS molecules that do not have the polymeric O-antigen, so-called rough LPS.[23] Recently we analysed the LPS structure of the genome strain Pm70 that exhibited a rough LPS structure.[24] The latter study also suggested that the LPS contained variation in the Kdo region of the molecule. This study was carried out on another strain of *Pm*, VP161, a highly virulent serotype A:1 strain, in order to gain further insight into *Pm* LPS structure and to examine if the variability in the Kdo region was also present in this strain. We had previously characterised the core OS of a heptosyltransferase mutant in VP161,[15,16] and here we report the complete structure for the LPS, including the novel arrangement in the Kdo region of the LPS molecule.

2. Results

Sugar analysis of the purified LPS and 8K pellet material revealed glucose (Glc), galactose (Gal) and L-*glyc*-

Table 1. Negative-ion CE–MS data and proposed compositions of O-deacylated LPS (LPS-OH) and core OS from *P. multocida* strain VP161[a]

Strain	$[M-3H]^{3-}$	$[M-4H]^{4-}$	Observed molecular ion	Calculated molecular ion	Lipid A size	Core OS size	Proposed composition
VP161	992.0	744.0	2979.5	2977.6	952	2025.6	2PCho, 3Hex, 4Hep, 2Kdo, Lipid A-OH
LPS-OH	999.0	749.0	2999.5	2999.5	952	2047.5	2PCho, 4Hex, 4Hep, Kdo-P, Lipid A-OH
	1033.0	774.0	3101.0	3100.7	1075	2025.7	2PCho, 3Hex, 4Hep, 2Kdo, Lipid A-OH
	1040.0	780.0	3123.5	3122.6	952	2170.6	2PCho, 4Hex, 4Hep, Kdo-P-PEtn, Lipid A-OH
	1040.0	780.0	3123.5	3122.6	1075	2047.6	2PCho, 4Hex, 4Hep, Kdo-P, Lipid A-OH
	1081.0	810.0	3245.0	3245.6	1075	2170.6	2PCho, 4Hex, 4Hep, Kdo-P-PEtn, Lipid A-OH
			$[M+2H]^{2+}$				
VP161		901.8	1805.6	1805.4	—		2PCho, 3Hex, 4Hep, Kdo
Core OS		982.9	1967.8	1967.6	—		2PCho, 4Hex, 4Hep, Kdo

[a] Average mass units were used for calculation of molecular mass based on proposed composition as follows: Hex, 162.15; Hep, 192.17; Kdo, 220.18; PEtn, 123.05; Lipid A-OH, 952.00.

ero-D-*manno*-heptose (LD-Hep) in the approximate ratio of 2:1:4, respectively. A small amount of *N*-acetyl-glucosamine (GlcNAc) was also identified. GLC analysis of the core oligosaccharide (OS) derived butylglycosides revealed Glc and Gal to be the D-isomers.

LPS-OH was prepared from LPS of fermenter-grown cells and analysed by CE–MS (Table 1). Triply charged ions were observed at *m/z* 992.0, 999.0 and 1040.0, corresponding to a composition of 2PCho, 4Hep, 3Hex, 2Kdo, Lipid A-OH for the smallest molecule. As shown below, the larger glycoforms corresponded to molecules with a phosphate molecule in place of the second Kdo residue, one more hexose residue in the core oligosaccharide, and for the largest glycoform (*m/z* 1040.0), an additional PEtn residue on the Kdo-P. Following growth on chocolate agar plates, additional glycoforms were indicated from triply charged ions of *m/z* 1033.0 and 1081.0 (Table 1). MS/MS analysis revealed that two different lipid A-OH species were found in the mixture of glycoforms, a basal species with a molecular mass of 952 amu as indicated by doubly and singly charged ions of *m/z* 475.5 and 951.5 following MS/MS, and a species containing an additional PEtn residue by virtue of a doubly charged ion of *m/z* 536.5 observed following MS/MS (Fig. 1c). The O-deacylated lipid A basal species (952 amu) consists of a disaccharide of N-acylated (3-OH C 14:0) glucosamine residues, each residue being substituted with a phosphate molecule. The larger lipid A species was only observed from plate-grown cells for the triply charged ions *m/z* 1033.0, 1040.0 and 1081.0. Additionally, evidence for the moiety P-PEtn was observed following MS/MS on glycoforms corresponding to the triply charged ions *m/z* 1040.0 and 1081.0 by virtue of a singly charged ion with *m/z* 219.5 (Fig. 1c). This ion was not observed following MS/MS on the triply charged ions of *m/z* 992.0, 999.0 and 1033.0. Furthermore MS/MS experiments revealed the size of the core OS molecules. For the triply charged ion at *m/z* 992.0, the core OS was 2027 amu as indicated by a doubly charged ion of *m/z* 1012.5 (Fig. 1a). This corresponds to a composition of 2Kdo, 2PCho, 4Hep, 3Hex. For the triply charged ion at *m/z* 999.0, the core OS was 2049 amu as indicated by a doubly charged ion of *m/z* 1023.5 (Fig. 1b). This corresponds to a composition of Kdo, P, 2PCho, 4Hep, 4Hex. For the triply charged ion at *m/z* 1040.0, the core OS was observed at 2172 amu as indicated by a doubly charged ion of *m/z* 1084.5 or inferred to be 2049 amu as indicated by a doubly charged ion of *m/z* 536.5 that corresponds to a basal lipid A species with an additional PEtn residue (Fig. 1c). This ion at *m/z* 1040.0 therefore corresponds to isomeric glycoforms that have either the P-PEtn moiety on Kdo or the additional PEtn on lipid A as evidenced by the two diagnostic doubly charged ions for the two lipid A species at *m/z* 475.5 and 536.5. As is often the case, evidence for the

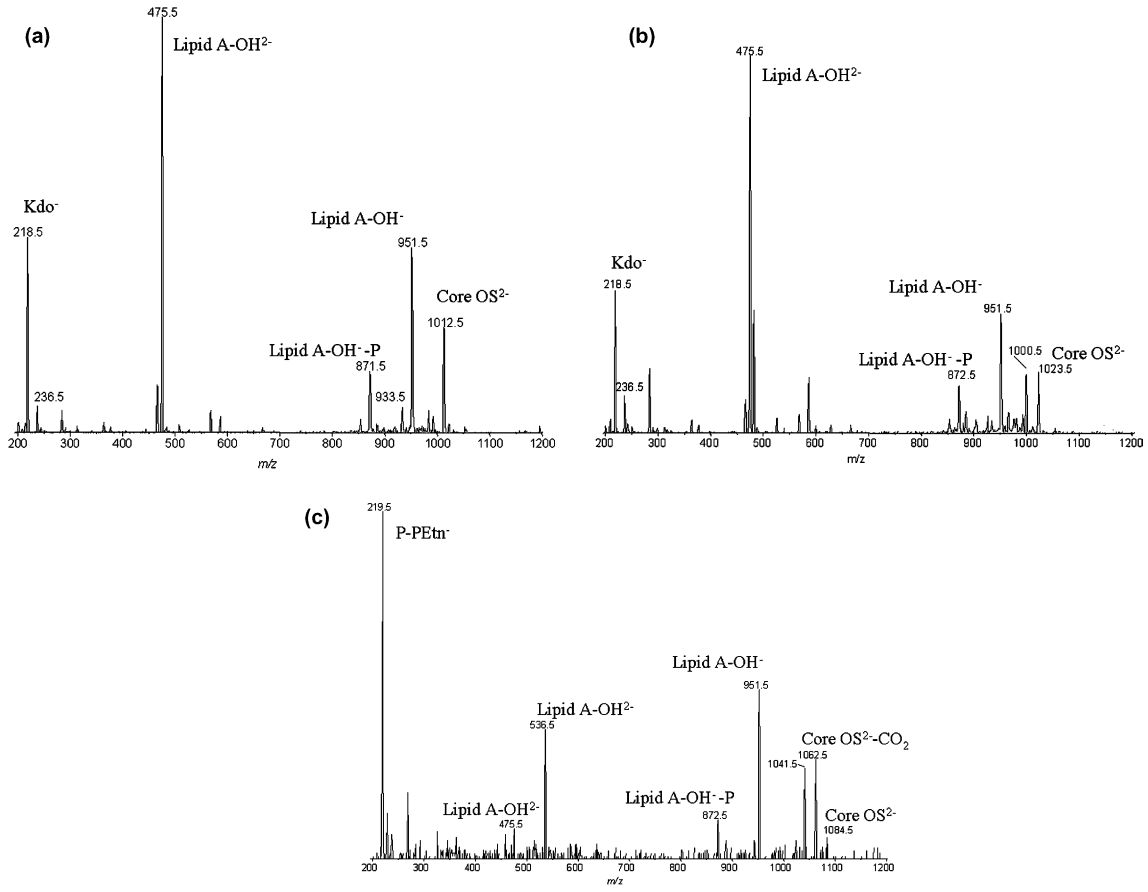

Figure 1. Negative-ion capillary electrophoresis–electrospray-ionisation mass spectra of the LPS-OH from *Pm* strain VP161. (a) Product ion spectrum from *m/z* 992^{3-}, (b) product ion spectrum from *m/z* 999^{3-}, (c) product ion spectrum from *m/z* 1040^{3-}.

loss of CO_2 from Kdo on MS/MS analysis was also observed.

MS analysis on the core oligosaccharides alone (derived from both LPS and 8K pellet material; giving the same spectra) revealed different fragmentation patterns from the doubly charged positive ions at *m/z* 903.0 and 984.0, which correspond to the doubly charged negative ions at *m/z* 902.0 and 983.0 in Table 1, consistent with the presence or absence of a hexose residue at the proximal heptose residue (Hep I) to Kdo. MS/MS on the doubly charged ion of *m/z* 903 (Fig. 2a) revealed a fragmentation pattern consistent with the absence of a Hex residue at Hep I. MS/MS on the doubly charged ion of *m/z* 984 (Fig. 2b) revealed that the larger OS had an additional hexose residue when compared to the former, and this hexose residue was located on the Hep I residue as shown by the presence of a doubly charged ion at *m/z* 682.0 and the absence of this signal, but the presence of the doubly charged ion *m/z* 697.0 following MS/MS of *m/z* 903.0 (Fig. 2a). Taken together this data suggests a novel mixture of glycoforms produced by VP161 LPS, some of which contain one Kdo species with a phosphate or pyrophosphoethanolamine moieties attached and another population that contains two Kdo molecules. In the species that contain two Kdo molecules, a hexose residue was not present at the proximal heptose residue of the core OS suggesting that biosynthesis of this arrangement is not possible. The location of the PCho residues was also determined from these MS/MS experiments in the positive-ion mode. A doubly charged ion of *m/z* 424.5 was found to correspond to a composition of 2PCho, 2Hex and Hep, and subsequent MS/MS/MS on this doubly charged ion revealed singly charged ions of *m/z* 328.5 and 520.5 corresponding to PCho–Hex and PCho–Hex–Hep, respectively, suggesting that two PCho–Hex moieties were attached to a Hep residue (Fig. 2c).

Methylation analysis was performed on the O-deacylated LPS (LPS-OH) in order to determine the linkage pattern of the molecule. Revealed were the presence of terminal Glc, 6-substituted Glc, terminal LD-Hep, 2-substituted LD-Hep and 4,6-disubstituted LD-Hep in the approximate molar ratio of 1:1:1:1:1, with lesser amounts of terminal Gal, 3,4-disubstituted LD-Hep and 3,4,6-trisubstituted LD-Hep being observed. Following HF treatment to remove phosphate residues that preclude optimal release of phosphorylated sugars on

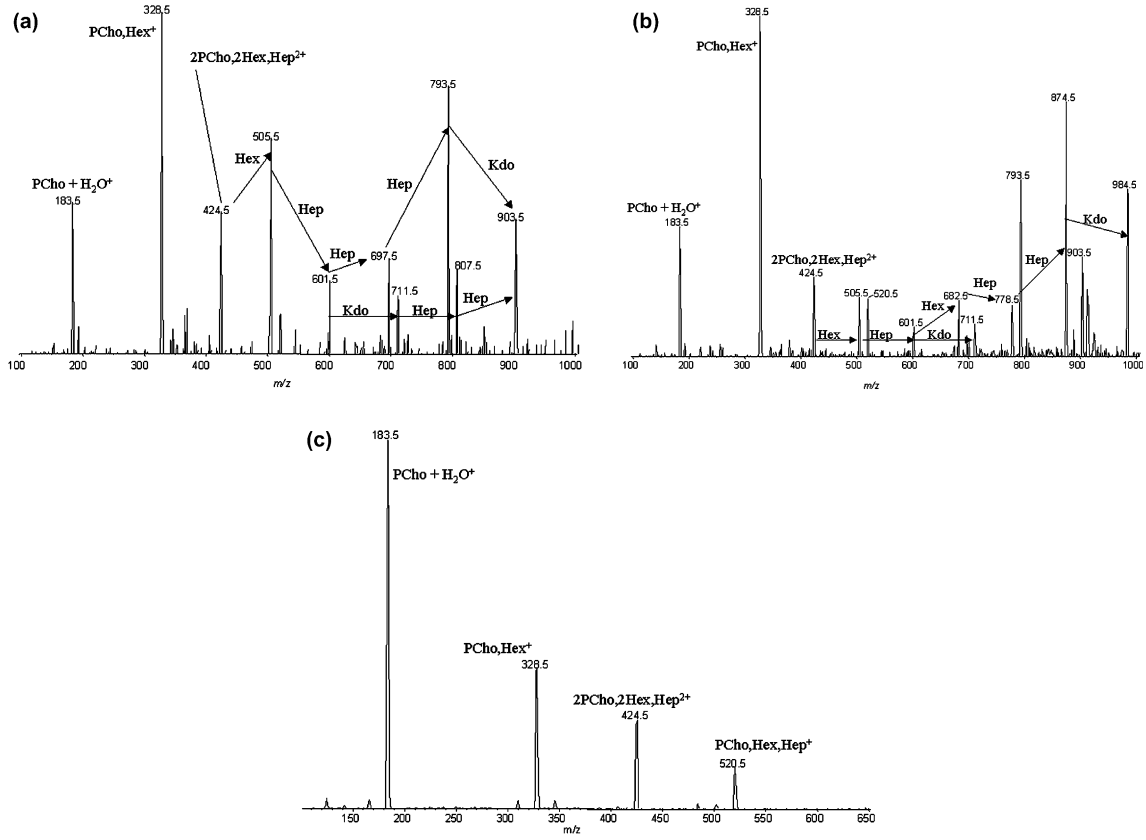

Figure 2. Positive-ion capillary electrophoresis–electrospray-ionisation mass spectra of the core OS from *Pm* strain VP161. (a) Product ion spectrum from *m/z* 903^{2+}, (b) product ion spectrum from *m/z* 984^{2+}, (c) product ion spectrum from *m/z* 424^{2+} utilising a high-orifice voltage.

hydrolysis, methylation analysis was repeated, which revealed the same sugars in the same ratio apart from the t-Gal residue that was now double the amount of the other components, suggesting that the PCho residues had been substituting Gal sugars.

In order to elucidate the exact locations and linkage patterns of the OS, NMR studies were performed on the OS fraction that gave the most resolved and homogeneous spectra. The assignment of ^{1}H resonances of the OS sample was achieved by COSY and TOCSY experiments with reference to the structurally related core OS from *P. multocida* strain Pm70[24] and from the related species *Mannheimia haemolytica*[25] and *Actinobacillus pleuropneumoniae*[26] (Table 2). The inner core residues (to Hep IV (f/f′)) were linked identically to the inner-core from the recently studied *P. multocida* strain Pm70,[24] and the assignments listed in Table 2 were consistent with that. However, there was no PEtn residue at the 3-position of Hep II (b) in the VP161 core OS. Interestingly for the core OS sample, the presence or absence of the Glc II residue (e) at Hep I (a) led to the identification of two sets of signals for the remaining inner core residues (Fig. 3). The two signals for Glc I at 4.64 (d) and 4.51 (d′) ppm were identified by NOE contact to the 4- and 6-positions of Hep I (a) as has been described previously; however, the absence of an inter-NOE contact between the anomeric proton resonances of Glc II (e) and the Glc I residue (d′) at 4.51 ppm identified the spin system for this Glc I residue (d′) when Glc II was absent. Conversely the presence of an inter-NOE contact between the anomeric proton resonances of Glc II (e) and the Glc I residue at 4.64 ppm (d) identified the spin system for this Glc I residue (d) when Glc II (e) was present (Fig. 3). This inter-anomeric NOE contact has been observed previously in the LPS of Pm70[24] and the related species *M. haemolytica*[25] and *Actinobacillus pleuropneumoniae*.[26] In such a way it was possible to assign the remaining inner core residues based upon the presence or absence of Glc II (e). The location and identification of the hexose residues at Hep IV (f/f′) remained to be elucidated. MS analysis had indicated that both hexose residues were substituted with PCho residues and were both substituting Hep IV (f/f′). The increased amount of t-Gal identified in methylation analysis following HF treatment concurred with this and suggested that the hexose residues bearing PCho were both Gal sugars. Two β-configured Gal residues, Gal I and Gal II, were identified in the core OS sample at 4.70 (g) and 4.66 (h) ppm, respectively, by virtue of their coupling constants and characteristic spin systems to H-4. The linkage positions of Gal I (g) and Gal II (h) at Hep IV (f/f′) were inferred from a NOESY

Table 2. ^{1}H and ^{13}C NMR chemical shifts for the core OS and fully deacylated (KOH treated) LPS from *Pasteurella multocida* VP161

	H-1	H-2	H-3	H-4	H-5	H-6	H-7	H-8	NOE's		
									Inter	Intra	Long range
α-GlcN[a]	5.75	3.47	3.93	3.53	4.13	4.31					
(x)	(92.7)	(55.1)	(70.5)	(70.7)	(73.7)	3.90					
						(70.2)					
β-GlcN[a]	4.88	3.17	3.92	3.94	3.78	3.75					
(y)	(100.0)	(56.6)	(72.8)	(75.3)	(74.9)	3.59					
						(63.4)					
Kdo[a]	—	—	2.37	4.62	4.29	3.84	3.77	3.96			
(z)			2.06	(71.2)	(72.9)	(nd)	(70.3)	3.72			
			(35.0)					(64.6)			
Hep-I[a] (a)	5.18	4.13	4.01	4.19	4.19	4.11	nd		4.29 Kdo H-5	4.09 H-2	
	(100.4)	(71.3)	(75.2)	(75.2)	(72.8)	(81.5)	nd				
							(nd)				
Hep-I[b] (a)	5.07	4.09	3.96	4.20	3.78	4.13	3.88		nd	4.09 H-2	
	(101.9)	(71.3)	(73.9)	(74.7)	(72.9)	(80.3)	3.75				
							(62.9)				
Hep-I[b] (a′)	5.01	4.15	4.04	4.26	nd	4.05	nd		nd	4.15 H-2	
	(101.4)	(71.3)	(73.9)	(74.2)	(nd)	(nd)	nd				
							(64.2)				
Hep-II[a] (b)	5.62	4.26	3.90	3.90	3.63	4.07	3.72		5.14 Hep III H-1	4.19 H-2	3.75 Hep I H-5
	(100.7)	(80.8)	(70.9)	(67.8)	(72.4)	(69.7)	3.62		3.96 Hep I H-3		
							(64.6)				
Hep-II[b] (b)	5.70	4.19	3.86	3.84	3.55	4.05	3.76		5.14 Hep III H-1	4.19 H-2	3.75 Hep I H-5
	(100.1)	(80.5)	(70.7)	(67.6)	(72.8)	(70.3)	3.65		3.96 Hep I H-3		
							(64.5)				
Hep-II[b] (b′)	5.76	4.17	3.85	3.83	3.60	4.05	3.76		5.11 Hep III H-1	4.17 H-2	3.76 Hep I H-5
	(99.7)	(80.5)	(70.7)	(67.6)	(72.8)	(70.3)	3.65		4.04 Hep I H-3		
							(64.5)				
Hep-III[c] (c)	5.11	4.01	3.87	3.83	3.78	4.05	3.77		5.76 Hep II H-1	4.01 H-2	3.94 Hep IV H-3
	(102.4)	(71.4)	(70.8)	(67.0)	(71.6)	(70.3)	3.65		4.17 Hep II H-2		3.59 Glc I H-4
							(64.9)				
Hep-III[b] (c′)	5.14	4.02	3.87	3.83	3.78	4.05	3.77		5.70 Hep II H-1	4.02 H-2	3.94 Hep IV H-3
	(102.4)	(71.4)	(70.8)	(67.0)	(71.6)	(70.3)	3.65		4.19 Hep II H-2		3.57 Glc I H-4
							(64.9)				
β-Glc-I[c] (d)	4.64	3.54	3.40	3.59	3.51	4.09	—		4.20 Hep I H-4	3.51 H-5	5.20 Glc II H-1
	(104.3)	(74.2)	(77.6)	(70.5)	(74.6)	3.76			4.13 Hep I H-6	3.40 H-3	
						(65.8)					
β-Glc-I[b] (d′)	4.51	3.53	3.42	3.57	3.57	4.05	—		4.26 Hep I H-4	3.57 H-5	
	(104.2)	(74.2)	(77.7)	(70.5)	(74.7)	3.83			4.05 Hep I H-6	3.42 H-3	
						(65.6)					
α-Glc-II[c] (e)	5.20	3.58	3.81	3.58	3.91	3.93	—		4.13 Hep I H-6	3.58 H-2	4.64 Glc I H-1
	(102.6)	(72.8)	(73.8)	(69.4)	(72.4)	3.74					
						(60.4)					
Hep-IV[c] (f)	4.95	4.17	3.93	4.19	3.91	4.32	3.97		4.09 Glc I H-6	4.17 H-2	
	(99.9)	(70.1)	(71.0)	(77.2)	(70.3)	(79.9)	3.75		3.77 Glc I H-6		
							(64.0)				
Hep-IV[b] (f′)	4.93	4.16	3.93	4.19	3.91	4.32	3.97		4.04 Glc I H-6	4.16 H-2	
	(99.9)	(70.1)	(71.0)	(77.2)	(70.3)	(79.9)	3.75		3.83 Glc I H-6		
							(64.0)				
β-Gal-I[b] (g)	4.70	3.69	4.19	4.12	3.80	nd	—		4.19 Hep IV H-4	4.19 H-3	
	(103.2)	(71.0)	(78.5)	(68.6)	(75.7)	nd				3.80 H-5	
						(nd)					
β-Gal-II[b] (h)	4.66	3.73	4.18	4.11	3.76	nd	—		4.32 Hep IV H-6	4.18 H-3	
	(104.5)	(71.0)	(78.5)	(68.6)	(75.5)	nd				3.76 H-5	
						(nd)					
PCho-I	4.38	3.68	3.22								
	(60.4)	(66.8)	(54.7)								
PCho-II	4.38	3.68	3.21								
	(60.4)	(66.8)	(54.7)								

[a] Data from KOH treated LPS is from the single Kdo residue containing glycoform.
[b] Data from core OS sample.
[c] Data from both KOH treated LPS and core OS, assignments identical. Data from Gal-I and Gal-II for the KOH treated LPS is not included due to considerable heterogeneity introduced by hydrolysis and migration of PCho residues.

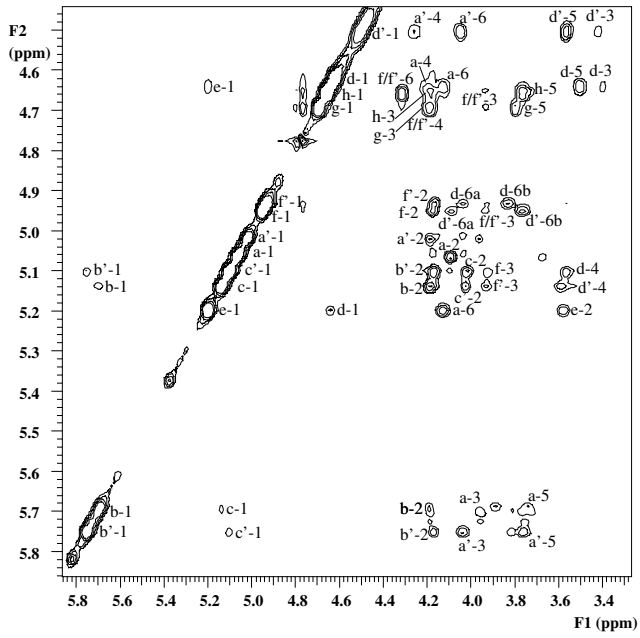

Figure 3. Region of the 2D-NOESY NMR spectrum of the core OS from *Pm* strain VP161. Letter designations for each residue are as indicated in the Abstract and in Table 2. The spectrum was recorded in D_2O at pH 7.0 and 25 °C with a mixing time of 400 ms.

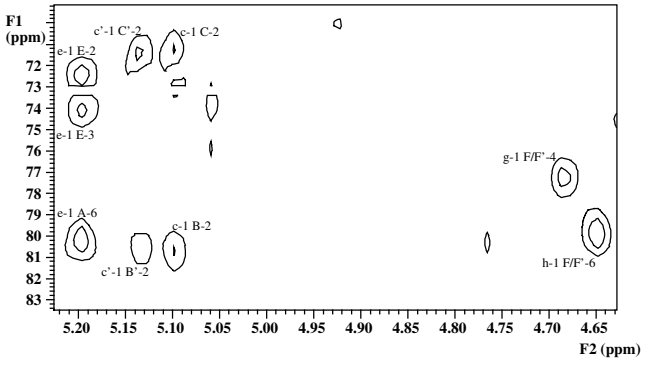

Figure 4. Region of the 2D ^{13}C–^{1}H-HMBC NMR spectrum of the core OS from *Pm* strain VP161 showing correlations between anomeric ^{1}H-resonances (lower case letters) and ring ^{13}C-resonances (upper case letters). The spectrum was recorded in D_2O at pH 7.0 and 25 °C.

experiment that indicated that the Gal I residue (g) was linked to the 4-position of Hep IV (f) and the Gal II residue was linked to the 6-position of Hep IV (f/f′) (Fig. 3). These inferences were confirmed from a ^{13}C–^{1}H-HMBC experiment that also confirmed the other linkages in the core OS (Fig. 4). In order to identify the locations of the two PCho residues, ^{31}P–^{1}H-HSQC and ^{31}P–^{1}H-HSQC–TOCSY experiments were performed that identified the previously assigned 3-positions of each Gal sugar as the point of attachment of each PCho residue (Fig. 5). This was confirmed by a ^{13}C–^{1}H-HMQC experiment, which identified the chemical shifts of the C-3 atoms of each Gal residue at low-field values (~78 ppm), which is consistent with phosphorylation.

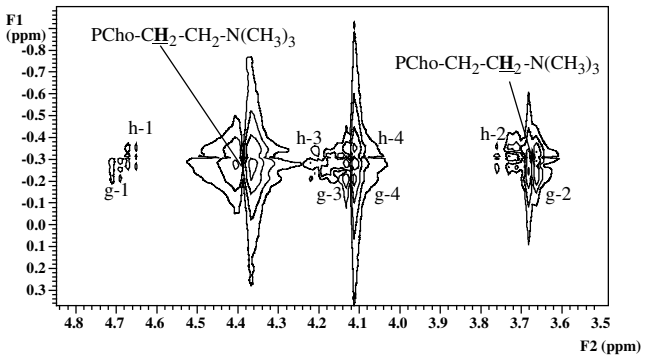

Figure 5. Region of the 2D ^{31}P–^{1}H-HSQC–TOCSY NMR spectrum of the core OS from *Pm* strain VP161 showing correlations between the ^{31}P-resonances (*x*-axis) and ^{1}H-resonances (*y*-axis) for the galactose residues labelled g-1 to g-4 and h-1 to h-4 and the choline resonances. The spectrum was recorded in D_2O at pH 7.0 and 25 °C.

In order to explore further the novel arrangements in the Kdo region of the molecule, deacylated samples were examined following KOH treatment. It was possible to separate fully deacylated LPS fractions that contained one and two Kdo residues (Fig. 6a and b). The presence of one and two Kdo residues containing glycoforms is clearly illustrated in Figure 6, as only one equatorial and one axial signal are visible for the H-3 protons of Kdo in Figure 6a (z_{3e} and z_{3a}), compared to two sets of signals for the equatorial and axial protons in Figure 6b (z_{3e}, z_{3a} and z'_{3e} and z'_{3a}). Complete assignment was possible for the one Kdo-containing sample, and partial assignment was only possible for the two Kdo residue-containing samples due to smaller amounts of this glycoform being available, resulting in a less intense spectrum. However, a rudimentary examination of the anomeric

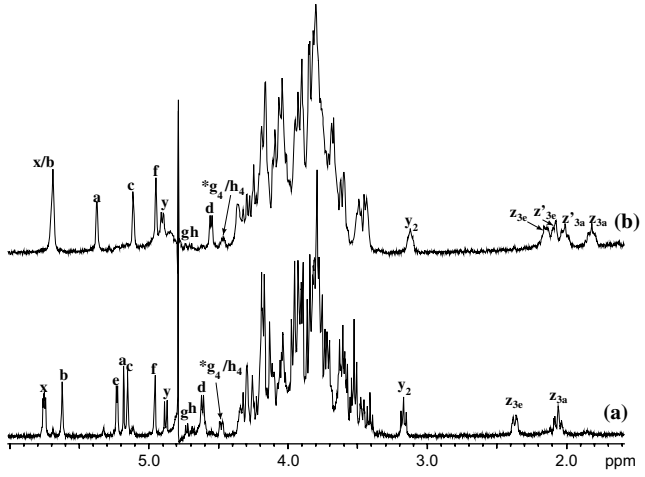

Figure 6. ^{1}H NMR spectra of the fully deacylated LPS from *Pm* strain VP161: (a) glycoform containing one Kdo residue; (b) glycoform containing two Kdo residues. The spectra were recorded in D_2O at pH 7.0 and 25 °C. Letter designations for each residue are as indicated in the Abstract and in Table 2. *Low-field shifts for the H-4 proton resonances of Gal I (g) and Gal II (h) are due to hydrolysis and migration of PCho residues during KOH treatment.

regions of the two spectra plainly shows the presence of a signal for the Glc II residue (e) in Figure 6a (where only one Kdo residue is present) and the absence of such a signal in Figure 6b (where two Kdo residues are present). As indicated by the core OS data, the presence or absence of the Glc II residue has an effect on the chemical shifts of several of the other anomeric proton resonances, particularly the Hep I (a), Hep II (b) and Glc I (d) signals, which is consistent with an effect on the conformation of the inner core molecule. Assignments for the one Kdo-containing glycoform are detailed in Table 2, which confirmed the assignments based on the core OS sample and extended this to include the Kdo-Lipid A region for the one Kdo-containing glycoform.

3. Discussion

Structural analysis of the oligosaccharide of the VP161 strain of *P. multocida* (*Pm*) has revealed a structure with similarities to and differences from the previously determined LPS core oligosaccharide structures for the genome strain Pm70 of *Pm*[24] and the related species *M. haemolytica* (*Mh*)[25] and *A. pleuropneumoniae* (*App*).[26] In each case the core OS contains an identically linked tri-heptosyl unit, that is, attached to a Kdo residue. Interestingly in Pm70 the 3-position of the HepII residue is substituted in the majority of cases with a PEtn residue, whereas in strain VP161 and in the related species *App* and *Mh*, no inner-core PEtn residues were observed. Apart from this variation in the substitution of Hep II with PEtn, both *Pm* strains and the related veterinary species *Mh* and *App* share a relatively conserved inner core structure. The only other differences in the inner core structure of *Pm* are the identification of an L-*glycero*-D-*manno*-configured heptose residue in the extension from the Glc I residue at Hep I compared to the D-*glycero*-D-*manno*-configured heptose residues encountered in *App* and *Mh*, and the variable presence of the Glc II residue in the *Pm* inner core, apparently due to the variability of the Kdo region of the molecule. This Glc II residue was stoichiometrically found in the inner core LPS of *App* and *Mh*. A different extension beyond this conserved inner core region was observed in strain VP161, whereby the Hep IV residue was disubstituted with two PCho-Gal moieties at the 4- and 6-positions. To our knowledge this structural arrangement has not been observed previously. It is rare to encounter two PCho residues in the same LPS molecule; non-typable *Hi* carriage strains 11 and 16 are the only documented examples of such an arrangement.[27] The presence of PCho residues could be implicated in the virulence of the *Pm* organism, as a role for PCho in adherence and colonisation in the respiratory tract has been documented.[28] It was also found that a mutant of strain VP161 that presented a truncated LPS structure lacking the two PCho residues was attenuated in both a mouse model and in chickens.[15,16] A previous study by other authors[17] had also observed a decrease in virulence of a *galE* mutant serotype D strain of *Pm* that could be due to alteration of the LPS structure. The most intriguing aspect of the VP161 LPS structure, however, is the variation observed in the Kdo region where both one Kdo and two Kdo-containing glycoforms have been observed. Additionally the impact on the inner core structure, that is, the presence or absence of Glc II at Hep I, caused by the variability of the Kdo region arrangement is interesting. The α-(1→6)-glucosyltransferase responsible for the transfer of Glc II to the Hep I residue is not known. It was interesting to note that only one homologue to Kdo transferases was identified in the *Pm* genome of strain Pm70 whose LPS also contained populations with both one Kdo and two Kdo-containing species.[24] It would also be of interest to compare the sequence of the Kdo transferase genes from *Pm*, *App* and *Mh* in order to investigate any sequence differences that could be attributed to the 'bi-functional' nature of the *Pm* transferase or if other regulatory factors are involved in this variability. This study has identified the LPS structure of a second *Pm* strain. Both strains share a similar inner core structure but a variable outer core decoration, and both exhibit an interesting variation in the Kdo region of the molecule, the significance of which remains to be investigated.

4. Experimental

4.1. Media and growth conditions

P. multocida strain VP161 was initially grown for 16 h on a chocolate agar plate at 37 °C, and growth was used to inoculate 1 L of brain–heart infusion (BHI) medium supplemented with β NAD (Sigma N-7004) to a final concentration of 5 μg/mL, haemin (Sigma H-2250) to a final concentration of 5 μg/mL and 1% glucose (10 g). Cultures were then incubated at 37 °C at 200 rpm for 6 h and used to inoculate the fermenter. *P. multocida* strain VP161 was then grown in a 28 L fermenter in 24 L of BHI broth for 18 h at 37 °C with 20% DO saturation. The cells were killed by addition of phenol to 2%, and 3 h post-phenol addition 1 g of hyaluronidase (Roche Chemicals) was added and stirred for 1 h before harvesting cells by using a Sharpless continuous flow centrifuge (~210 g).

4.2. Isolation, purification and degradation of the lipopolysaccharide

P. multocida cells (~210 g wet wt) were freeze-dried, yielding ~56 g. Freeze-dried cells were washed with organic solvents (1 × ethanol, 2 × acetone, 2 × light petro-

leum ether) to remove lipids and other lipophilic components to enhance the efficiency of the LPS extraction.[29] Washed cells (10 g from ~42 g) were extracted by the hot phenol–water method,[30] and the aq phases were combined and dialysed against running water for 48 h. The retentate was freeze-dried yielding ~1.6 g, made up to a 2% solution in water and treated with DNase and RNase at 37 °C for 4 h, followed by proteinase K treatment at 37 °C for 4 h. Small peptides were removed by dialysis. After freeze-drying, the retentate (~0.2 g) was made up to a 2% solution in water, centrifuged at 8000*g* for 15 min (yielding an 8K pellet of ~85 mg), followed by further centrifugation of the supernatant at 100,000*g* for 5 h. The pellet, containing purified LPS, was redissolved and freeze-dried (yielding ~17 mg). The 8K pellet material (~40 mg) was treated with anhydrous hydrazine with stirring at 37 °C for 1 h to prepare O-deacylated LPS (LPS-OH). The reaction mixture was cooled in an ice bath, and gradually, cold acetone (−70 °C, five vols.) was added to destroy excess hydrazine, and the precipitated LPS-OH was isolated by centrifugation and lyophilisation of the redissolved pellet (~35 mg). The sample was then purified down a Bio-Gel P-2 column with individual fractions lyophilised. The core oligosaccharide (OS) was isolated by treating separately the 8K pellet material (~45 mg) and the LPS (~17 mg) with 1% acetic acid (10 mg/mL, 100 °C, 1.5 h), with subsequent removal of the insoluble lipid A by centrifugation (5000*g*). The lyophilised OS sample from the 8K pellet was subsequently further purified down a Bio-Gel P-2 column as above. Fully deacylated LPS was isolated by treatment of LPS-OH (~12 mg) with 4 N KOH at 125 °C for 16 h, and following neutralisation it was fractionated by anion-exchange liquid chromatography as described previously.[29]

4.3. Analytical methods

Sugars were determined as their alditol acetate derivatives[31] by GLC–MS. Samples were hydrolysed for 4 h using 4 M trifluoroacetic acid at 100 °C. The hydrolysate was reduced ($NaBD_4$) for 16 h in H_2O and acetylated with Ac_2O at 100 °C for 2 h using residual sodium acetate as catalyst. The GLC–MS was equipped with a 30 M DB-17 capillary column (180–260 °C at 3.5 °C/min), and MS was performed in the electron-impact mode on a Varian Saturn II mass spectrometer. Methylation analysis was carried out by the NaOH–DMSO–methyl iodide procedure[32] and analysed by GLC–MS as above. Absolute configurations were determined by GLC analysis of butyl glycoside derivatives.[26]

4.4. Mass spectrometry (MS)

ESIMS was performed in the negative-ion mode on a VG Quattro Mass Spectrometer (Micromass, Manchester, UK) by direct infusion of samples in 25% aq acetonitrile containing 0.5% acetic acid. Capillary electrophoresis–mass spectrometry (CE–MS) was performed on a Prince CE system (Prince Technologies, The Netherlands) coupled to an API 3000 mass spectrometer (Applied Biosystem/Sciex, Concord, Canada) via a microspray interface. A sheath solution (2:1 2-propanol–MeOH) was delivered at a flow rate of 1 μL/min to a low-dead-volume tee (250 μm i.d., Chromatographic Specialties). All aqueous solutions were filtered through a 0.45-μm filter (Millipore) before use. An electrospray stainless steel needle (27 gauge) was butted against the low-dead-volume tee and enabled the delivery of the sheath solution to the end of the capillary column. The separations were obtained on about 90 cm length bare fused-silica capillary using 10 mM ammonium acetate–ammonium hydroxide in deionised water, pH 9.0, containing 5% MeOH. A voltage of 20 kV was typically applied at the injection. The outlet of the capillary was tapered to ca. 15 μm i.d. using a laser puller (Sutter Instruments). Mass spectra were acquired with dwell times of 3.0 ms per step of 1 *m*/*z* unit in full-mass scan mode. The MS/MS data were acquired with dwell times of 1.0 ms per step of 1 *m*/*z* unit. Fragment ions formed by collision activation of selected precursor ions with nitrogen in the RF-only quadrupole collision cell were mass analysed by scanning the third quadrupole.

4.5. Nuclear magnetic resonance (NMR) spectroscopy

NMR experiments were carried out on Varian Inova 400, 500 and 600 MHz spectrometers using a 5-mm or 3-mm triple resonance (^1H, ^{13}C, ^{31}P) probe. The lyophilised sugar sample was dissolved in 600 μL (5 mm) or 140 μL (3 mm) of 99% D_2O. The experiments were performed at 25 °C with suppression of the HOD (deuterated H_2O) signal at 4.78 ppm. The methyl resonance of acetone was used as an internal reference at 2.225 ppm for ^1H spectra and 31.07 ppm for ^{13}C spectra. Standard homo- and heteronuclear correlated 2D pulse sequences from Varian, COSY, TOCSY, NOESY, ^{13}C–^1H HSQC, ^{13}C–^1H HSQC–TOCSY and ^{13}C–^1H HMBC were used for general assignments. The 1D ^{31}P experiment was carried out on a Varian Inova 200 spectrometer with a sweep width of 40 ppm, 20,000 transients and acquisition time of 1.6 s. The 2D ^1H–^{31}P HSQC experiment was acquired on a Varian Inova 400 spectrometer for 6 h. The coupling constant was optimised at 10 Hz by performing an array of 1D-HSQC experiments. The sweep width in the *F*2 (^1H) dimension was 6.0 ppm and in the *F*1 (^{31}P) dimension was 16.2 ppm. Water presaturation during the relaxation delay was 1.5 s, acquisition time in t_2 was 0.21 s, and 32 increments with 180 (HMQC) scans per increment were obtained. The 2D ^1H–^{31}P HSQC–TOCSY experiment was acquired on a

Varian Inova 400 spectrometer for 8 h using the same parameters as the HSQC experiment with a TOCSY mixing time of 150 ms.

Acknowledgements

The authors would like to thank Perry Fleming for cell growth, Lisa Morisson for mass spectrometry, and Prof. Ben Adler for providing strain VP161.

References

1. Christensen, J. P.; Bisgaard, M. *Rev. Sci. Technol.* **2000**, *19*, 626–637.
2. De Alwis, M. C. *Br. Vet. J.* **1992**, *148*, 99–112.
3. Chanter, N. *Can. J. Vet. Res.* **1990**, *54*, S45–S47.
4. Weber, D. J.; Wolfson, J. S.; Swartz, M. N.; Hooper, D. C. *Medicine (Baltimore)* **1984**, *63*, 133–154.
5. Boyce, J. D.; Adler, B. *Infect. Immun.* **2000**, *68*, 3463–3468.
6. Galdiero, M.; Folgore, A.; Nuzzo, I.; Galdiero, E. *Immunobiology* **2000**, *202*, 226–238.
7. Horadagoda, N. U.; Hodgson, J. C.; Moon, G. M.; Wijewardana, T. G.; Eckersall, P. D. *Res. Vet. Sci.* **2002**, *72*, 194–200.
8. Mendes, S.; Carmichael, K. P.; Nunnally, J. C.; Glisson, J. R.; Cheng, I. H.; Harmon, B. G. *Avian Dis.* **1994**, *38*, 790–796.
9. Rhoades, K. R.; Rimler, R. B. *Avian Dis.* **1987**, *31*, 523–526.
10. Ganfield, D. J.; Rebers, P. A.; Heddleston, K. L. *Infect. Immun.* **1976**, *14*, 990–999.
11. Brogden, K. A.; Rebers, P. A. *Am. J. Vet. Res.* **1978**, *39*, 1680–1682.
12. Rebers, P. A.; Phillips, M.; Rimler, R.; Boykins, R. A.; Rhoades, K. R. *Am. J. Vet. Res.* **1980**, *41*, 1650–1654.
13. Wijewardana, T. G.; Wilson, C. F.; Gilmour, N. J.; Poxton, I. R. *J. Med. Microbiol.* **1990**, *33*, 217–222.
14. Ramdani, X.; Adler, B. *Vet. Microbiol.* **1991**, *26*, 335–347.
15. Harper, M.; Boyce, J. D.; Wilkie, I. W.; Adler, B. *Infect. Immun.* **2003**, *71*, 5440–5446.
16. Harper, M.; Cox, A. D.; St.Michael, F.; Boyce, J. D.; Wilkie, I. W.; Adler, B. *Infect. Immun.* **2004**, *72*, 3436–3443.
17. Fernandez de Henestrosa, A. R.; Badiola, I.; Saco, M.; Perez de Rozas, A. M.; Campoy, S.; Barbe, J. *FEMS Microbiol. Lett.* **1997**, *154*, 311–316.
18. Rosner, H.; Grimmecke, H. D.; Knirel, Y. A.; Shashkov, A. S. *Carbohydr. Res.* **1992**, *223*, 329–333.
19. DeAngelis, P. L.; Gunay, N. S.; Toida, T.; Mao, W. J.; Linhardt, R. J. *Carbohydr. Res.* **2002**, *337*, 1547–1552.
20. Namioka, S. *Methods Microbiol.* **1978**, *10*, 271–291.
21. Heddleston, K. L.; Gallagher, J. E.; Rebers, P. A. *Avian Dis.* **1972**, *16*, 925–936.
22. Carter, G. R.; Chengappa, M. M. Am. Assn. Vet. Lab. Diagnos. *24th Annual Proceedings*, 1981; pp 37–42.
23. Rimler, R. B. *J. Clin. Microbiol.* **1990**, *28*, 654–659.
24. St. Michael, F.; Vinogradov, E.; Li, J.; Cox, A. D. *Glycobiology*, in press.
25. Brisson, J.-R.; Crawford, E.; Uhrin, D.; Khieu, N. H.; Perry, M. B.; Severn, W. B.; Richards, J. C. *Can. J. Chem.* **2002**, *80*, 949–963.
26. St. Michael, F.; Brisson, J.-R.; Larocque, S.; Monteiro, M.; Li, J.; Jacques, M.; Perry, M. B.; Cox, A. D. *Carbohydr. Res.* **2004**, *339*, 1973–1984.
27. Landerholm, M.; Li, J.; Richards, J. C.; Hood, D. W.; Moxon, E. R.; Schweda, E. K. H. *Eur. J. Biochem.* **2004**, *271*, 941–953.
28. Weiser, J. N.; Pan, N.; McGowan, K. L.; Musher, D.; Martin, A.; Richards, J. C. *J. Exp. Med.* **1998**, *187*, 631–640.
29. Masoud, H.; Moxon, E. R.; Martin, A.; Krajcarski, D.; Richards, J. C. *Biochemistry* **1997**, *36*, 2091–2103.
30. Westphal, O.; Jann, K. *Methods Carbohydr. Chem.* **1965**, *5*, 88–91.
31. Sawardeker, D. G.; Sloneker, J. H.; Jeanes, A. *Anal. Chem.* **1965**, *37*, 1602–1604.
32. Ciucanu, I.; Kerek, F. *Carbohydr. Res.* **1994**, *131*, 209–217.